Numerical and experimental investigations of bistable beam snapping using distributed Laplace force

A. Amor, Amâncio Fernandes, J. Pouget

Noname manuscript No.
(will be inserted by the editor)

Numerical and experimental investigations of bistable beam snapping using distributed Laplace force

A. Amor · A. Fernandes · J. Pouget

Received: date / Accepted: date

Abstract We report a study of an elastic buckled beam undergoing a contactless magnetic actuation of Laplace type. The beam model is based on the elastica beam theory including the beam extensibility. The Laplace force is produced by an electric current travelling along the beam placed in a magnetic induction. The magnitude of the electric current is the control parameter and by increasing the electric current the beam switches from one stable state to the other one for a given beam end-shortening.
The main purpose of the study is to investigate the bistable response, more precisely, the diagram of the electric current as function of the midpoint vertical displacement of the beam according to the magnet location along the elastic beam. The model equations are established and they are numerically solved using an algorithm developed for nonlinear boundary value problem.
A second part of the study is devoted to experimental validation of the model and comparisons with the results extracted from the numerical solutions to the model equations. Especially, the comparisons ascertain with good accuracy the approach of the proposed bistable beam model. In addition, the influence of the model parameters on the bistable response is clearly identified.

Keywords Bistable mechanism · buckling · snap-through · Laplace force · bifurcation · experimental tests

A. Fernandes
Sorbonne Université, CNRS, Institut Jean le Rond d'Alembert, UMR 7190, F-75005 Paris, France
E-mail: amancio.fernandes@sorbonne-universite.fr

1 Introduction

In previous work the switching mechanism of an elastic bistable beam due to the Laplace force actuation was reported in [1]. In this work, the authors have presented (i) a beam model based on the elastica theory for slender beams, (ii) the actuation mechanism produced by the Laplace force, (iii) the numerical solutions to the model equations and (iv) the experimental validations of the bistable response subject to the Laplace force. In the study the magnetic induction produced by the magnets are placed parallel to the whole length of the beam. It means that the bistable beam was subject to the lineic density of force upon the entire length of the beam.
In the proposed study, we want to know what would be the bistable response if the length of the pair of the magnets is less than the total length of the beam. In this situation, the lineic density of the Laplace force is partly distributed over a section of the beam. Consequently, new configurational parameters must be considered, namely, the magnet length and the position of the magnet center. More precisely, a question may be raised, is there an (or several) optimal location(s) of the magnets for which the electric current traveling in the beam is less than any other position?

One of the advantages of the bistable mechanism is that it requires low energy during the switching process from one stable configuration to the other one. Another advantage in actuation application is that they can be displayed in large strokes compared to straight and monostable structures. Both buckled beams and elastic arches possess this attractive property that allows them to be used in a large variety of applications in the area of micro and nano-electromechanical systems

(MEMS/NEMS) [2–7].
Many applications in advanced technological devices continue to attract the attention of engineering researches such as micro-positioners, switches, valves, relays [8,9], tactile display [10,11], and mechanical memory for data storage [12]. Most research works proposed in the literature have been focused on the use of static forces to produce the transition between the two stable states involving the inherent instability of the buckled beams. Those driving forces (extended to applied moments) can be mechanical [4, 13–16], magnetic [17, 18], thermal [19,20] including actuation using shape memory alloys [21] or electrostatic [22–25]. A bistable smart beam model has been proposed by [26], the author examine the snap-trough action of a bistable beam equipped with piezoelectric actuators. An experimental validation is presented as well. Among the numerous applications of bistable beam, a special attention has been paid to applications involving bistable mechanisms to microrobotics [27]. Some promising devices have been proposed, for instance, bistable gripper [28]. An interesting and comprehensive review of buckled structures has been reported by [29], going from simple buckled beams or shallow elastic arches to morphing structures such as elastic shells, multistable cylinder lattices including the combination of multiple bistable beams for deployable structures. Some studies using electro-thermal actuation has been considered to control the axial force of bistable micro-beams [30] for application to flow velocity sensors. Such an electro-thermal actuation has been used for the snap-through of a pre-shaped double beams with opposite curvatures [31]. To close the present list of applications, we can quote the study of a buckled beam equipped with piezoelectric sensors for energy harvesting [32]. In the present work, we want to analyze the complex and the rich response of the buckled elastic beam under an electromagnetic actuation. More precisely, the chosen actuation is the Laplace force [33, 34] produced by an electric current traveling along the beam (in conductive material, metal) placed in magnetic induction.

The proposed model is based on the elastica theory of elastic beams [35–38]. Such an approach is particularly rich because the kinematic description accounts for large transformations of the beam (cross-section rotation of large amplitudes). Many studies analyzed in the literature have proposed alternative modeling for kinematic description and for the nonlinear response of the buckled beam in its post-buckling regime. Among the different approaches found in literature some are based on the modal projection, that is the solution to the equations of the buckled beam expanded on the base formed by the buckling modes. Vangbo [39] has proposed interesting detailed analysis of the snap-through effect of the bistable buckled beam. His model accounts for the compressibility of the elastic beam for small deflections. Based on the modal projection model, a study of the snap-through and bistability of beams with arbitrarily pre-shaped deformation has been examined by [40]. Stability and bifurcation conditions are discussed in details. In other respects, a weakly nonlinear approach has been examined by [41]. The authors have carried out a model in which the nonlinearity is due to the coupling between deflection and beam stretching (geometrical nonlinear deformation). A study of the behaviour of post-buckled beams has been conducted by Jiao *et al.* [42] based on small (modal projection) and large transformation (elastica) models. Extension to shallow elastic arches has been considered using this kind of approach [43, 44]. A more sophisticated model has been conducted by [45], the authors consider the strain gradient formulation of the elasticity to model bistable beams or shallows arches under electrostatic actuation.

The chosen beam model is presented in the next section (Section 2). Especially, in this section, the beam kinematics is described by two strain measures which are the extensional strain along the beam axis and the beam curvature. Both descriptions in the fixed frame and local frame attached to the deformed beam are given in the same section. The model is based on previous work [1] and is briefly recalled in Section 3. Moreover, the boundary conditions - clamped-clamped beam - and continuity conditions at the magnet boundaries are specified in the same section. Section 4 deals with the numerical study of the nonlinear boundary value problem. The numerical problem thus stated relies on the model equations based on the shooting method associated with a numerical procedure to capture the unknown shooting parameters. One of the main results coming from the numerical investigations is the bistable response, in other words, the actuating driving force (or the electric current) as a function of the beam midpoint displacement. The results are discussed according to the chosen parameters (magnet position, the end-shortening). A part of the work is devoted to the experimental validations of the proposed model reported in Section 5, the results thus obtained are discussed and compared with those deduced from the model.

2 Description of the system and modeling

2.1 Deformation measures, resultants in force and moment

We consider a clamped-clamped initially straight elastic beam $[AB]$ of length L_0, width b, and thickness h. The beam is isotropic and homogeneous. A fixed reference frame $\mathcal{R}_0\,\{A;\boldsymbol{e}_1,\boldsymbol{e}_2,\boldsymbol{e}_3\}$ is attached to the fixed point A of the beam and the basis vector $\boldsymbol{e}_1$ coincides with the beam axis in its state of rest. The beam transformation takes place in the $\{\boldsymbol{e}_1,\boldsymbol{e}_2\}$ plane. Fig.1.a gives a sketch of the beam in its configuration at rest. The left clamp is fixed while the right clamp undergoes a small end-shortening ΔL caused by an axial compressive force. The distance between both clamps is now $L = L_0 - \Delta L$ (Fig.1.b). A material point G of the beam located at the curvilinear abscissa s measured along the deformed beam is considered. A local frame is attached at the current point $G\,(s)$ of the beam and it is defined by $\{G;\boldsymbol{\tau},\boldsymbol{n},\boldsymbol{e}_3\}$ where $\boldsymbol{\tau}$ is the unit vector tangent to the deformed beam, $\boldsymbol{n}$ is the unit vector perpendicular to $\boldsymbol{\tau}$ and $\boldsymbol{e}_3$ is identical to that of the fixed referential.
Accordingly, the position of the material point G is given by

$$\boldsymbol{AG} = \boldsymbol{q}\,(s) = x(s)\boldsymbol{e}_1 + y(s)\boldsymbol{e}_2\,, \quad s\in[0,L_0]\,, \tag{1a}$$

$$= q_T\,(s)\,\boldsymbol{\tau} + q_N\,(s)\,\boldsymbol{n}\,, \tag{1b}$$

either in the fixed frame or the local frame. We are able to compute the relationship between the coordinate $\{x,y\}$ and $\{q_T,q_N\}$ using the rotation of the beam cross-section $\theta = (\boldsymbol{e}_1,\boldsymbol{\tau})$. The beam kinematics are reported in detail in [1]. The different frame vectors and coordinates are shown in Fig.1.b. The rectangular shaded in clear grey displayed in Fig.1.b is the magnet that produces the magnetic induction in the $\boldsymbol{e}_3$ direction. Fig.1.c is the top view of the beam exhibiting both magnets and the abscissa of their center and length.

The deformation measures describing the beam deformation from its state at rest to the actual configuration are the curvature $\kappa = \frac{d\theta}{ds}$ and the extensional strain given by $\varepsilon = \Lambda - 1$ where $\Lambda = \frac{d\bar{s}}{ds}$ is the ratio of the length of differential line element of the beam in the deformed configuration to that of the undeformed one. The actuation mechanism of the bistable beam is modelled by a uniform density of lineic force which is nonetheless permanently perpendicular to the deformed beam. Such an actuation is produced by Laplace force. In the present study the magnetic induction is applied only on a part of the beam length (see Fig.1.b and Fig.1.c).

We consider a density of electric current per volume unit $\boldsymbol{j}$ running through an elementary volume dv of the beam. The latter is placed in a magnetic induction field $\boldsymbol{\mathcal{B}}$. According to the classical electrodynamics [34] the infinitesimal Laplace force acting onto the elementary volume of the beam takes on the form

$$\boldsymbol{dF} = \boldsymbol{j}\times\boldsymbol{\mathcal{B}}\,dv\,, \tag{2}$$

We recall that the beam cross-section is rectangular, its area is given by $\mathcal{A} = b\,h$. The elementary volume is then given by $dv = \mathcal{A}d\ell$ (where $d\ell$ is an elementary length of the beam). On using now the electric current per unit of length denoted by i such that $i\boldsymbol{\tau} = \mathcal{A}\boldsymbol{j}$, the elementary Laplace force reads as

$$\boldsymbol{dF} = i\,d\ell\,\boldsymbol{\tau}\times\boldsymbol{\mathcal{B}}\,. \tag{3}$$

The magnetic induction field $\boldsymbol{\mathcal{B}}$ in the present situation is produced by two identical magnets placed on both side of the beam (see Fig.1.b and 1.c). Moreover, the magnetic induction is supposed to be uniform in the volume defined by the magnets.
The internal force within the beam cross-section is $\boldsymbol{R} = (N,T)$ where N is the axial force, and T is the shear force, and the bending moment is $M\boldsymbol{e}_3$. The internal actions (forces and moment) are depicted in Fig.1.d.

2.2 Model equations

The equations of the model are deduced from the principle of virtual work accounting for the boundary conditions at the ends of the beam. The set of the equilibrium equations in dimensionless notation takes on the following form (the reader is welcome to refer to [1])

$$\mathsf{N}' - \theta'\mathsf{T} = 0\,, \tag{4a}$$

$$\theta'\mathsf{N} + \mathsf{T}' - \mathsf{f} = 0\,, \tag{4b}$$

$$\mathsf{M}' + (1+\varepsilon)\,\mathsf{T} = 0\,. \tag{4c}$$

Along with the above equations, we must consider the geometrical compatibility relationships deduced from the definition of the tangent vector to the deformed beam. These equations written in the local frame are

$$Q_T' - \theta' Q_N - (1+\varepsilon) = 0\,, \tag{5a}$$

$$Q_N' + \theta' Q_T = 0\,, \tag{5b}$$

where Q_T and Q_N are the tangential and normal displacements, respectively. We recall that $\boldsymbol{Q} = \boldsymbol{q}/L_0$. At last, we write down the constitutive equations for the internal actions (in dimensionless notation)

$$\theta' - \mathsf{M} = 0\,, \tag{6a}$$

$$\varepsilon - k\,\mathsf{N} = 0\,, \tag{6b}$$

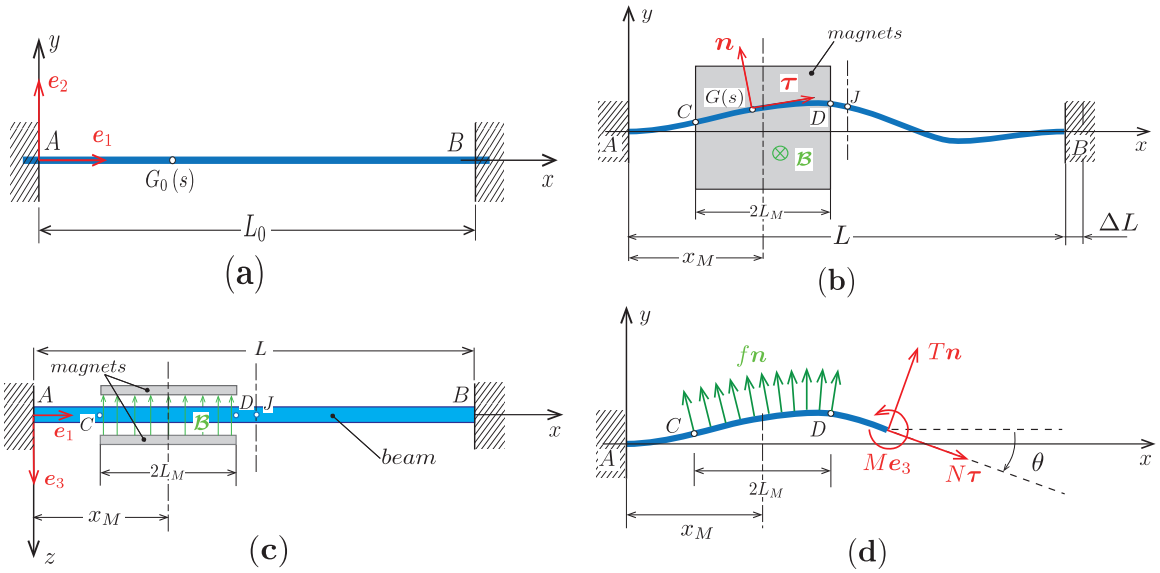

Fig. 1 Bistable beam : (a) beam at rest in the reference configuration, (b) buckled beam and magnetic actuation and (c) top view (d) internal and external actions on the beam.

where the prime is the derivative with respect to the dimensionless curvilinear abscissa S defined by $S = \frac{s}{L_0}$ and k characterizes the beam extensibility the latter is given, in present case, by $k = \frac{h^2}{12L_0^2}$. The dimensionless variables have been used by introducing appropriate characteristic force and moment (see [1]). For sake of consistency, we briefly recall how the dimensionless variables have been defined in the previous study $(\mathsf{f}, \mathsf{N}, \mathsf{T}, \mathsf{M}) = (fL_0/F_0, N/F_0, T/F_0, M/M_0)$. The reference force and moment are given by $F_0 = E\mathcal{A}k$, and $M_0 = EI/L_0$, respectively (E is the Young modulus and I is the moment of inertia of the cross-section with respect to $\boldsymbol{e}_3$ direction). We notice, here, that the force $\boldsymbol{f} = f\,\boldsymbol{n}$ is a lineic density of force with $f = i.\mathcal{B}$ deduced from Eqns. (3) (see Fig.1.d).

2.3 Boundary and continuity conditions

For sake of convenient, we introduce the following vector

$$\boldsymbol{\xi}(S) = \begin{bmatrix} \theta(S) \\ Q_N(S) \\ Q_T(S) \end{bmatrix} . \tag{7}$$

On using the above notation, the boundary conditions associated to the beam equations take on the form (clamp condition)

$$\boldsymbol{\xi}(0) = \mathbf{0}\,, \qquad \boldsymbol{\xi}(1) = \begin{bmatrix} 0 \\ 0 \\ X_B \end{bmatrix} , \tag{8}$$

where X_B is the abscissa of the right point B after end-shortening. The clamping actions are unknown.

The magnets are placed only on a part of the beam length (see Fig. 1), the applied lineic force is defined on three domains such as

$$\mathbf{f}(S) = \mathbf{0} \qquad S \in [0, S_C[\cup]S_D, 1]\,, \tag{9a}$$
$$\mathbf{f}(S) = \mathsf{f}\,\boldsymbol{n} \qquad S \in [S_C, S_D]\,. \tag{9b}$$

The abscissa S_C and S_D are defined as the intersection of the deformed beam with vertical limits on the left side and right side of the magnets referred as to their abscissas X_C and X_D, respectively, and they are

$$X(S_C) = X_C \qquad \text{and} \qquad X(S_D) = X_D\,. \tag{10}$$

Moreover, we have

$$X_C = X_M - \mathsf{L}_M \qquad \text{and} \qquad X_D = X_M + \mathsf{L}_M\,, \tag{11}$$

where X_M is the dimensionless abscissa of the middle location of the pair of magnets and $2\mathsf{L}_M$ is their length. In addition, some continuity conditions at the boundaries of the domain must be satisfied at S_C and S_D

$$[\![\boldsymbol{\xi}(S_C)]\!] = \mathbf{0} \qquad \text{and} \qquad [\![\boldsymbol{\xi}(S_D)]\!] = \mathbf{0}\,. \tag{12}$$

In Eqns. (12), the double square braces hold for the discontinuity defined by $[\![\boldsymbol{\xi}]\!] = \boldsymbol{\xi}^+ - \boldsymbol{\xi}^-$ at the point to be considered. On using the notations introduced in (7), equations (12) amount to saying that the variables θ, Q_N and Q_T are continuous at the material points S_C and S_D.

3 Computing bistable response under actuation and results

Now, we have all the ingredients of the mechanical system to investigate the response of the bistable beam subject to the Laplace force. The latter is applied to a localized zone of the beam length as depicted in Fig.1.b and Fig.1.c. The first task is to solve the boundary value problem described by the set of Eqns. (4,5 and 6), by using a shooting method. The numerical simulations for bistable beam equations are based on the algorithm described in the previous study [1]. In this study the accuracy of the model equation was validated by a finite element computation on the $1D$ model. Accordingly, the model equations given by Eqns. (4) will be considered in the forthcoming sections.

The main numerical problem to overcome is the existence of unstable branches in the bistable response. In these zones we are faced with the divergence of the numerical algorithm and the discrepancy of the results could be arisen. In order to get around such a problem an efficient way of solving correctly the model equation is to control the displacement of a material point of the beam. We control the crossing point of the beam and a fixed vertical line located at the mid-point between the beam ends A and B and such that $Q_X(S_J) = (1 - \Delta\mathsf{L})/2$ (in dimensionless unit), where S_J is the curvilinear abscissa of the crossing point J (referred to Fig.1). Therefore, the idea is to increment the vertical coordinate of the mid-point $Q_Y(S_J) = Y_J$ by a very small amount at each iteration. Accordingly, the numerical algorithm provides a unique deformed beam while the beam is switching.

The numerical results are performed for an elastic thin beam made of an amagnetic stainless steel $A316L$ having a Young modulus $E = 207$ GPa. The beam dimensions are the length 200 mm, the width 10 mm, and the thickness 0.2 mm. The magnetic induction between both magnets is about 0.2 Tesla. The numerical method allows us to compute the density of Laplace force due to the magnetic induction and the electric current is then computed from Eqn. (3) leading to $i = \frac{\|\boldsymbol{f}\|}{\|\boldsymbol{\mathcal{B}}\|}$. The first result is the response of the bistable beam, more precisely, the electric current as a function of the mid-point displacement (referred as to J, see Fig.1.b) $y_m = Y_J L_0$ according to the magnet location.

Fig. 2 shows the numerical results for three magnet positions, (i) at 50% (magnets at the mid-point), (ii) at 38% from the fixed left end of the beam and (iii) at 24% (no far from the left point). The solid line corresponds to the stable zone while the dashed line refers to the unstable region of the switching process. We note that the

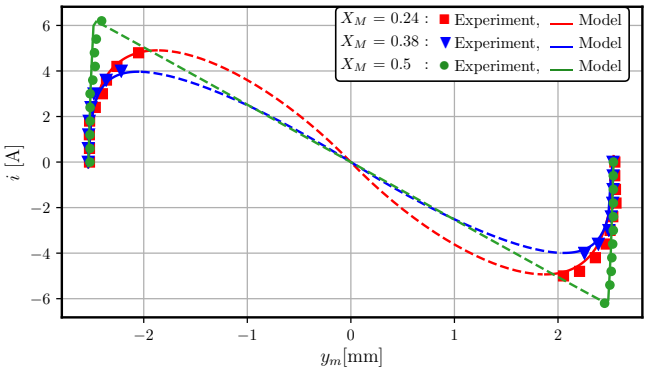

Fig. 2 Bistable response : electric current as a function of the beam mid-point displacement for three different values of the magnet position for a given end-shortening set at $\Delta\mathsf{L} = 0.04\%$ (in solid line : the elastica; points, triangles and squares : experimental results).

behavior of the bistable beam response is very sensitive to the magnet position. For the magnets at the middle of the beam ends an N-shaped curve is clearly observed. At first sight, the beam response for this symmetrical actuation is mainly characterized by the combination of the first three buckling modes. The bistable response is somewhat different for off-center actuation. In Fig. 2, for two different off-center actuations (0.24 and 0.38) we observe round-off of the curve when passing the maximum or minimum of the electric current. The non-symmetrical actuation promotes a bistable switching involving the first two buckling modes and the third mode playing substantially no role. For off-center actuation the maximum of electric current to produce the snap-through is less than that of mid-span actuation. Fig. 3 reports the variation of the electric current

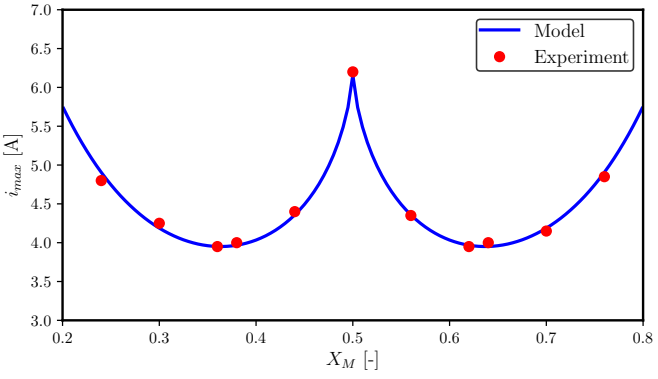

Fig. 3 Variation of the electric current maximum versus the position of the pair of magnets for $\Delta\mathsf{L} = 0.04\%$ (in solid line : the elastica; points : experimental results).

needed to produce switching as a function of the magnet location. It is clear that the curve is symmetric with

respect to the center. Nevertheless, there exists an optimal position of the magnets (the center of the pair of magnets) for which the electric current is minimum, i.e. around the off-center position 36.3%. However, once the length of the magnets no longer allows their center to be positioned in the vicinity of 36.3% ($2\mathsf{L}_M > 72.6\%$), the optimal configuration is such that the right or the left edge of the pair of the magnets is placed at either end of the beam. For $2\mathsf{L}_M = 80\%$ for instance the optimal position is $X_M^{opt} = 40\%$. In addition, Fig. 4 shows that two other parameters have an impact on the optimal position of the magnets. Indeed, looking at Fig. 4, the position corresponding to the minimum of the switching electric current X_M^{opt} increases as the end-shortening $\Delta\mathsf{L}$ and decreases as the slenderness L/h increases. The last series of numerical results are obtained by keeping the off-center actuation fixed and examining the influence of the end-shortening on the bistable beam response. The results are presented in Fig. 5 for three different end-shortening values (0.02%, 0.04% and 0.06%) leading to different mid-point deflections of the beam and maximums of the electric current.

4 Experimental validations

The present section reports a series of results extracted from the experimental tests performed on the bistable beam partly actuated by Laplace force. The experimental study is quite similar to that of the magnetic actuation along the entire length of the beam [1]. The experimental tests concern the results coming from the numerical solution to the bistable beam model, especially the electric current versus mid-point displacement according to the location of the pair of magnets for different end-shortening values. Comparisons with the results derived from the modeling study are discussed in details.

4.1 Technical details about the experimental set-up

4.1.1 Material

The thin elastic beams used for the experimental tests are described in the previous section. Nevertheless, a particular attention has been paid to obtain a high quality of planar beams with a minimum of residual stress. The magnetic induction field is produced by a pair of identical magnets of neodyme type ($NdFeB$ alloy) their dimensions are a length of 80 mm, a width of 17 mm, and a thickness of 5 mm.

4.1.2 Experimental set-up

Different views (global test bench, instruments of measurement) of the experimental set-up are shown in Fig. 6. The elastic thin beam is fixed at each of its end in a clamp. One end of the beam is fixed, the other one is placed on a travel translator stage equipped with a micro-metric screw. On moving the translator we are able to control the end-shorting of the beam with a 10 μm adjustment. In addition, the end-shortening is measured correctly thanks to a digital comparator. The beam is placed between the pair of magnets as described above. The pair of magnets is allowed to move parallel to the beam axis. A Gaussmeter equipped with Hall effect probe allows measuring the magnetic induction produced by the magnets, the magnetic induction found is about 0.2 Tesla. An electric current supply device is used to deliver a given stable current running through the beam. A power resistor is connected in series to secure the power supply. Nevertheless, we can ask ourselves what is the impact of the Joule effect produced by the electric current passing through the beam. The temperature rise is about $0.0916°C$ for a snap-through time of $50\,ms$. This variation of temperature gives rive to a beam elongation of $0.3\,\mu m$, which is small enough so that the effect is not noticeable in comparison to the beam imperfections and the accuracy of the measuring equipment. The experimental measurement process follows different steps : (i) the electric current is increased step by step from zero to the value which produces a strong enough Laplace force to trigger the beam snapping. For this value, the beam switches and gets the other stable position. (ii) The electric current is switched off as soon as the snap-through has been detected. (iii) The variation of the mid-point of the beam is measured using a laser profilometer (a Keyence® ultra-speed laser profilometer model LJ-V7060). (iv) The profilometer signal is sent to the computer in order to be analyzed and correlated to the input signal for the electric current. (v) The signal is converted into an analogical value for the displacement of the beam center. (vi) The test is then repeated for switching in the opposite direction.

4.2 Experimental results and analysis

Three main results are obtained and analyzed from the experimental data. Among the first results are the measurements of the bistable response for different positions of the pair of magnets for a given end-shortening. The experimental results are shown in Fig. 2. In order to make a comparison with the results coming from the model, the experimental points are superposed to

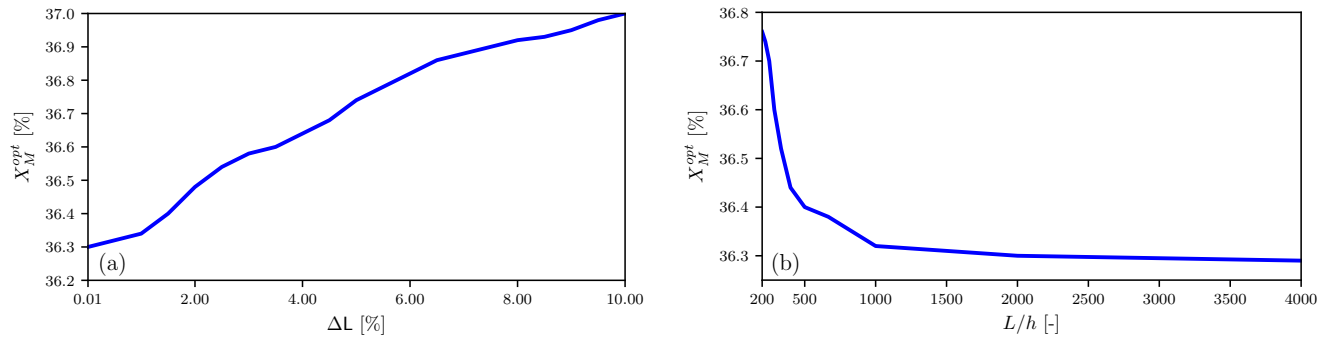

Fig. 4 The variations of the optimal actuating location X_M^{opt} for $2\mathsf{L}_M = 0.4$: (a) as a function of the end-shortening $\Delta\mathsf{L}$, and (b) as a function of the slenderness L/h.

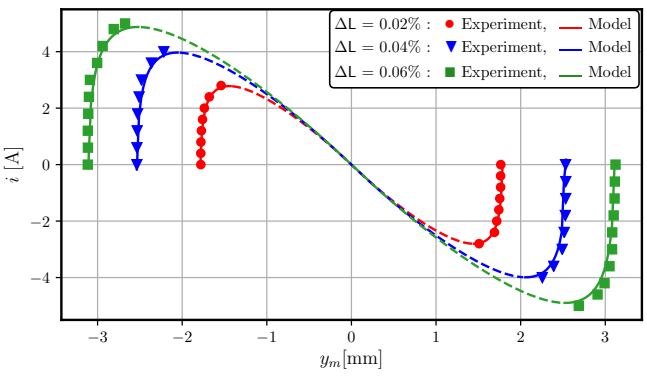

Fig. 5 Bistable response : electric current as a function of the beam mid-point displacement for three different values of the end-shortening for a given position (38%) of the pair of magnets (in solid line : the elastica; points, triangles and squares : experimental results).

the solid lines corresponding to the numerical results. The switching process has been performed in both directions from one stable position to the other one and *vise versa*. At first sight, we observe that the experimental points are very close to those obtained with the analytical study, the discrepancy is less than 3.4%. The experimental study obviously does not allow to obtain data in the unstable zone (dashed line for analytical results). It is worthwhile noting that for the off-center actuation the instability phenomena is shifted with respect to that of the mid-point actuation. The off-set increases as the location of the magnets is close to the beam ends.

The second series of results are obtained for a given off-set actuation when varying the end-shortening. Fig. 5 shows the experimental results (symbols in the figures) superposed to the curves extracted from the numerical results. Once again, the experimental study yields a clear validation of the numerical simulation performed using the model equations. The discrepancy between the experimental data and the results obtained with the numerical simulations does not exceed 2%.

The last results of the experimental study are illustrated in Fig. 3 exhibiting the variation of the maximum of electric current as a function of the position of the pair of magnets. The experimental data are referred as to the red points which are very close to the solid line for the analytical results. The optimal position for the pair of magnets is located at about 36.3% ($X_M = 0.363$). At this position, the maximum of the electric current is less than any other maxima. The value of the electric current is about 4 A. Nevertheless, the present result is certainly dependent on the bistable parameters such as the end-shortening as well as the magnet length. Moreover, it is noteworthy drawing a parallel between the present results and those issued from a similar work concerning the bistable beam actuation using a punctual force. An identical result, but in the case of a punctual force actuation, was already pointed out by Cazottes *et al.* [16] but on using the modal expansion method, and by Camescasse *et al.* [13] in the framework of the elastica approach of the beam theory. The minimum of the actuating force is not located at the beam mid-point. The exact position is very dependent on the beam slenderness and end-shortening (see Fig. 4).

5 Discussion and concluding remarks

The essential results of the present model of bistable beam actuation using a distributed Laplace force lie with the validation of the model by experimental tests. The model thus adopted is based on the elastica theory of elastic beams which accounts for displacements and rotations of large amplitudes. Moreover, the model includes the beam extensibility which plays a crucial role in the switching process. One of the originalities of the study is the distributed Laplace force actuation on a finite zone of the beam which is permanently perpendic-

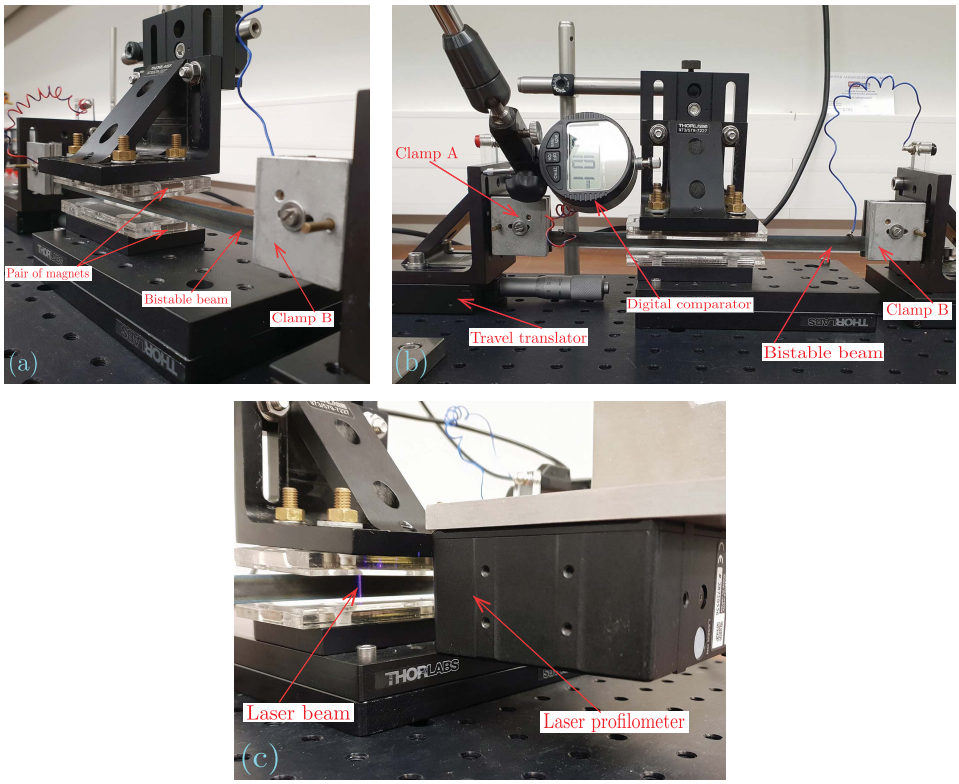

Fig. 6 Photos of the experimental set-up : (a) view showing the beam placed between the both magnets (b) the global view of the bistable buckled beam fixed with the clamps at each of its ends and different instruments and (c) the measurement of the mid-point beam displacement owing the laser profilometer.

ular to the deformed beam. The bistable beam response under Laplace force is investigated according to the position of the actuating zone (the center of the magnets) with respect to the beam length. In particular, the off-center actuation needs a maximum of electric current to have the beam switched smaller than that of the central position for a given end-shortening. The experimental results reported in the present study ascertain the numerical predictive results for the bistable beam response and the influence of the magnet location.

An optimal position of the pair of magnets has been placed in evidence. For an actuation localized at about 36.3% from the left or the right of the beam we have the minimum of the electric current producing the Laplace force for the beam switching. These results can be of relevant interest in engineering applications such as micro-switches, micro-robotics, tactile interfaces, or MEMS.

A natural extension of the present work and forthcoming work would be to study the vibration of the bistable beam in the post-buckling regime, for instance, vibrations of small amplitudes around the buckled state, in first time. However, one of the most interesting studies would be the nonlinear dynamical response of the bistable system under time-dependent excitation of the Laplace force type. Especially, the latter can be easily controlled by varying in time the electric current running through the beam [41, 44, 46]. The experimental validations of the vibrating behaviors of the buckled beam will be considered as well.

Acknowledgements The research work reported in the paper has been supported by the research project BISCELTECH funded by Fonds Unique Interministériel (FUI-APP21).

Conflict of interest

The authors declare that they have no conflict of interest.

References

1. Amor A., Fernandes A., Pouget J., Snap-through of elastic bistable beam under contactless magnetic actuation. Int. J. Non-Linear Mech. 119, 103358 (2020)
2. Buchaillot L., Millet O., Quevy E., Collard D., Post-buckling dynamic behavior of self-assembled 3D microstructures. Microsyst. Technol. 14, 69-78 (2008).
3. Casals-Terre J., Fargas-Marques A., Shkel A.M., Snap-action bistable micro-mechanisms actuated by nonlinear resonance. J. Microelectromech. Syst. 17, 1082-1093 (2008).

4. Qiu J., Lang J.H., Slocum A.H., A curved-beam bistable mechanism. J. Microelectromech. Syst. 13, 137-146 (2004).
5. Krylov S., Ilic B.R., Lulinsky S.: Bistability of curved microbeams actuated by fringing electrostatic fields. Nonlinear Dynamics 66, 403-426 (2011).
6. Seunghoon P., Dooyoung H., Pre-shaped buckled-beam actuators : Theory and experiments. Sens. Actuators A. Phys. 148, 186-192 (2008).
7. Saif M.T.A., On a tunable bistable MEMS - Theory and experiment. J. Microelectromech. Syst. 9, 157-170 (2000).
8. Chen G., Gou Y., Zhang A., Synthesis of compliant multistable mechanisms through use of a single bistable mechanism. J. Mech. Design., 133, 081007 (2011).
9. Fu S., Ding G., Wang H., Yang Z., Feng J., Design and fabrication of a magnetic bi-stable electromagnetic MEMS relay. Microelectronics J., 38, 556-563 (2007).
10. Hafez M.n Tactile interfaces : Technologies, applications and Challenges. Visual Compt., 23, 267-272 (2007).
11. Niu X., Broche P., Stoyanov H., Yu S.R., Pei Q., Bistable electroactive polymer for refreshable braille display with improved actuation stability. In Proc. of SPIE p.83400R1 (2012).
12. Roodenburg D., Spronck J.W., Van der Zant H.S.V., Venstra W.J., Buckling beam micromechanical memory with on-chip readout. Appl. Phys. Lett., 94, 183501 (2009).
13. Camescasse B., Fernandes A., Pouget J., Bistable buckled beam: Elastica modeling and analysis of static actuation. Int. J. Solids and Structures 50, 2881-2893 (2013).
14. Camescasse B., Fernandes A., Pouget J., Bistable buckled beam and force actuation : Experimental validations. Int. J. Solids and Structures 51, 1750-1757 (2014).
15. Cazottes P., Fernandes A., Pouget J., Hafez M., Design of actuation for bistable structures using smart materials. CIMTEC 2008, 3rd International Conference on Smart Materials, Structures and Systems, 8-13 June, 2008, Acireale, Sicily, Italy.
16. Cazottes P., Fernandes A., Pouget J., Hafez M., Bistable buckled beam : modeling and actuating force and experimental validations. ASME J. Mech. Des. 131, 1001001-1001011 (2010).
17. Han J.S., Ko J.S., Kim Y.T., Kwak B.M., Parametric study and optimization of micro-optical switch with a laterally driven electromagnetic microactuator. J. Micromech. Microeng. 12, 39-47 (2002).
18. Park S., Hah D. : Pre-shaped buckled-beam actuators, Theory and experiment. Sens. Actuators A. Phys., 148, 186-192 (2008).
19. Stanciulescu I., Mitchell T., Chandra Y., Eason T., Spottswood M., A lower bound on snap-through instability of curved beams under thermomechanical loads. Int. J. Non-linear Mech., 47, 561-575 (2012).
20. Alcheikh N., Ben Mbarek S., Ouakad H.M., Younis M.I., A highly sensitive and wide-range resonant magnetic microsensor based on a buckled micro-beam. Sensors and Actuators A: Physical, 328 (2021).
21. Zaidi S., Lamarque F., Prelle C., Carton O., Zeinert A., Contactless and selective energy transfer to a bistable micro-actuation using laser heated shape memory alloy. Smart Mater. Struct. 21, 115027 (14 pages) (2012).
22. Zhang Y., Wang Y., Li Z., Huang Y., Li D., Snap-through and pull-in instabilities of an arch-shaped beam under an electrostatic loading. J. Microelectromech. Syst., 16, 684-693 (2007).
23. Krylov S., Ilic B.R., Schreiber D., Saratensky S., Craighead H., The pull-in behavior of electrostatically actuated bistable microstructures. J. Micromech. Microeng. , 18, 055026-1-055026-20 (2008).
24. Das K., Batra R.C., Pull-in and snap-through instabilities in transient deformations of microelectromechanical systems. J Micromech. Microeng., 19, 035008-1-035008-19 (2009).
25. Younis M.I., Ouakad H.M., Alsaleem F.M., Miles R., Cui W., Nonlinear dynamics of MEMS arches under harmonic electrostatic actuation. J. Microelectromech. Syst., 19, 647-656 (2010).
26. Aimmanee S., Tichakorn K., Piezoelectrically induced snap-through buckling in a buckled beam bonded with a segmented actuator. J. of Intell. Mat. Sys. and Struct. (2018).
27. Hafez M., Lichter M.D., Dubowsky S., Optimized binary modular reconfigurable robotic devices. Mechatronics, IEEE/ASME Transactions, 8, 18-25 (2003).
28. Palathingal S., Ananthasuresh G.K.: Analysis and design of fixed-fixed bistable arch-profiles using a bilateral relationship. J. Mech. and Robotics, 11(3), 031002 (7 pages) (2019).
29. Hu N., Burgueño R., Buckling-induced smart applications: recent advances and trends. Smart Mat. Struct., 24(6) (2015).
30. Torteman B., Kessler Y., Liberzon A., Krylov S., Electrothermal excitation of parametric resonances in double-clamped micro beams. Appl. Phys. Let., 115(19) (2019).
31. Hussein H., Khan F. Younis M.I., A monolithic tunable symmetric bistable mechanism. Smart Mat. Struct., 29(7) (2020).
32. Xie Z., Kwuimy K.C.A., Wang Z., Huang W., A piezoelectric energy harvester for broadband rotational excitation using buckled beam. AIP Advances, 8(1) (2018).
33. Maugin G.A., Continuum mechanics of electromagnetic solids. North-Holland, Series Applied Mathematics and Mechanics, vol. 33 (Amsterdam, 1988).
34. Jackson, J.D., Classical electrodynamics (3rd ed.). John Wiley and Sons, New York (1998).
35. Love A.E.H., A Treatise on the Mathematical Theory of Elasticity. Dover Publications, fourth Edition, (1944).
36. Frasier C.G., Mathematical technique and physical conception in Euler's investigation of the elastica. Centaurus, 34, 211-246 (1991).
37. Antman S.S., Nonlinear Problems of Elasticity. Applied Mathematical Series 107 (2nd ed.). Springer-Verlag. (2005).
38. Magnusson A., Ristinmaa M., Ljung C., Behaviour of the extensible elastica solution. Int. J. Solids and Structures, 38, 8441-8457 (2001).
39. Vangbo M., An analytical analysis of a compressed bistable buckled beam. Sensors and Actuators A69, 212-216 (1998).
40. Hussein H., Younis M.I., Analytical study of the snap-through and bistability of beams with arbitrarily initial shape. J. Mechanisms Robotics, 12(4) (2020).
41. Nayfeh H., Emam S.A., Exact solution and stability of postbuckling configurations of beams. Nonlinear Dynamics 54, 395-408 (2008).
42. Jiao P., Alavi A.H., Borchani W., Lajnef N., Small and large deformation models of post-buckled beams under lateral constraints. Math. Mech. Solids 24 (2), 386-405 (2017).
43. Pinto O.C., Gonçalves P.B., Active non-linear control of buckling and vibrations of a flexible buckled beam. Chaos Solitons & Fractals. 14, 227-239 (2002).
44. Chandra Y., Stanciulescu I., Virgin L.N., Eason T.G. , Spottswood S.M., A numerical investigation of snap-through in a shallow arch-like model. J. Sound and Vibration, 332, 2532-2548 (2013).

45. Tajaddodianfar F., Pishkenari H.N., Yazdi M.R.H., Miandoab E.M., Size-dependent bistability of an electrostatically actuated arch NEMS based on strain gradient theory. J. Phys. D: Appl. Phys., 48(24) (2015).
46. Nayfeh N., Emam S.A., On the nonlinear dynamics of a buckled beam subjected to a primary-resonance excitation. Nonlinear Dynamics, 35, 1-17 (2004).